Biosensors and Bioelectronics 78 (2016) 221–228

Contents lists available at ScienceDirect

Biosensors and Bioelectronics

journal homepage: www.elsevier.com/locate/bios

Highly sensitive detection of urinary protein variations using tilted fiber grating sensors with plasmonic nanocoatings

Tuan Guo [a], Fu Liu [a], Xing Liang [b], Xuhui Qiu [a], Yunyun Huang [a], Chen Xie [b], Peng Xu [b], Wei Mao [b,*], Bai-Ou Guan [a,*], Jacques Albert [c]

[a] Guangdong Provincial Key Laboratory of Optical Fiber Sensing and Communications, Institute of Photonics Technology, Jinan University, Guangzhou 510632, China
[b] Guangdong Provincial Hospital of Chinese Medicine, Guangzhou 510120, China
[c] Department of Electronics, Carleton University, 1125 Colonel By Drive, Ottawa, Canada K1S 5B6

ARTICLE INFO

Article history:
Received 30 September 2015
Received in revised form
14 November 2015
Accepted 16 November 2015
Available online 17 November 2015

Keywords:
Fiber grating
Optical fiber
Biochemical sensor
Surface plasmon resonance
Urinary protein

ABSTRACT

Surface plasmon resonance (SPR) optical fiber biosensors can be used as a cost-effective and relatively simple-to-implement alternative to well established bulky prism configurations for high sensitivity biological sample measurements. The miniaturized size and remote operation ability offer them a multitude of opportunities for single-point sensing in hard-to-reach spaces, even possibly in vivo. The biosensor configuration reported in this work uses a tilted fiber Bragg grating (TFBG) in a commercial single mode fiber coated with a nanometer scale silver film. The key point is that by reducing the silver film thickness to around 20–30 nm (rather than 50 nm for optimal SPR excitation), different modes of the TFBG spectrum present very high but opposite sensitivities to refractive index (RI) changes around the TFBG. Experimental results obtained with the coated TFBG embedded inside a microfluidic channel show an amplitude sensitivity greater than 8000 dB/RIU (Refractive Index Unit) and a limit of detection of 10^{-5} RIU. Using this device, the effect of different concentrations of protein in rat urine was clearly differentiated between healthy samples, nephropatic samples and samples from individuals under treatment, with a protein concentration sensitivity of 5.5 dB/(mg/ml) and a limit of detection of 1.5×10^{-3} mg/ml. Those results show a clear relationship between protein outflow and variations in the RI of the urine samples between 1.3400 and 1.3408, pointing the way to the evaluation and development of new drugs for nephropathy treatments. The integration of TFBGs with microfluidic channels enables precise measurement control over samples with sub-microliter volumes and does not require accurate temperature control because of the elimination of the temperature cross-sensitivity inherent in TFBG devices. Integration of the TFBG with a hypodermic needle on the other hand would allow similar measurements in vivo. The proposed optical fiber/microfluidic plasmonic biosensor represents an appealing solution for rapid, low consumption and highly sensitive detection of analytes at low concentrations in medicine as well as in chemical and environmental monitoring.

1. Introduction

Human urine normally contains a few volume of protein that is less than 150 mg per 24 h and it is hard to be identified by routine tests. Proteinuria, defined as urinary protein excretion greater than 300 mg per 24 h, is an important sign for renal damage and its expression often precedes any detectable decline in renal filtration function. The increase of proteinuria accelerates kidney damage and promotes the progression of chronic kidney disease (CKD) and finally leads to end-stage renal disease (ESRD) (Ishani et al., 2006; Tonelli et al., 2011). Previous studies identify that proteinuria is a strong and independent predictor of the increased risk for cardiovascular mortality in CKD patients with or without diabetes (Agrawal et al., 2009; Matsushita et al., 2010). Therefore, early diagnosis of proteinuria is essentially important for prevention and treatment of chronic kidney disease and its complications. Traditional methods to identify the small changes in urine due to expression increasing of protein are conducted by detecting the protein excretion. The most widely accepted formats of “wet-lab” type analytic biochemistry assays are the Coomassie brilliant blue protein assay (Chial et al., 1993) and the bicinchoninic acid assay

* Corresponding authors.
E-mail addresses: maowei@gzucm.edu.cn (W. Mao), tguanbo@jnu.edu.cn (B.-O. Guan).

http://dx.doi.org/10.1016/j.bios.2015.11.047

(BCA) (Smith et al., 1985). These methods are commonly implemented using bulk optic laboratory instrumentation (like microplate array systems) in applications such as pharmaceutical research where a large number of tests performed simultaneously in parallel. However these methods are susceptible to environmental interferences and suffer from time consuming sample preparation (having to bring samples back to a laboratory and label the sample for additional selection and amplification). Designing new sensing techniques with detection levels and reliability comparable to large laboratory instruments, but using label-free methods in small scale point-of-care devices is an important development in this field.

The use of optical fiber devices as biomedical sensors presents many well-known desirable features (size, cost, feasibility) for label-free methods as they contribute to the overall reduction in costs and ease of use factors (Baldini et al., 2012; Wang and Wolfbeis, 2013). Fiber optic sensors can be easily inserted into the media to be sensed (instead of having to bring samples inside an instrument) either as a hand held probe or as a set of remotely operated devices along a fiber optic cable (in environmental monitoring applications for instance). However, it should be noted that for biochemical sensing fields, it is usually necessary to improve the limit of detection (LOD) levels to at least 10^{-5} RIU (Refractive Index Unit), by increasing the wavelength shift sensitivity while keeping noise level down and spectral features narrow (White and Fan, 2008). Fortunately, it has been recently demonstrated that the addition of a nanometric-scale gold or silver coating overlay on the optical fiber outer surface considerably enhances the refractometric sensitivity through the generation of surface plasmon resonance (SPR) (Homola, 2008; Piliarik and Homola, 2009; Shalabney and Abdulhalim, 2011; Caucheteur et al., 2015). The increased sensitivity achieved with plasmon waves arises because of the large localization of electromagnetic energy in the layer immediately adjacent to the metal surface. Any perturbation in that layer, such as the bonding of analytes on receptor molecules modifies the local refractive index (RI) of the dielectric and the plasmon phase velocity. Meanwhile, in order to effectively excite and accurately measure plasmon resonances and hence to achieve this optimum sensitivity, a new kind of fiber grating, i.e. the tilted fiber Bragg grating (TFBG, corresponds to a RI modulation angled by a few degrees relative to the perpendicular to the propagation axis) has been developed and well studied (Albert et al., 2013; Guo et al., 2014, 2016; Thomas et al., 2012; Caucheteur et al., 2013). TFBGs benefit from two unique features: the strong polarization selectivity of the excited cladding modes (coming from the breaking of the cylindrical symmetry of non-polarization-maintaining fibers) and the high-density comb of narrowband spectral resonances (available to excite SPR over a wide range of refractive indices and to measure their spectral location with quality factors between 10^3 and 10^4). Therefore, SPR based TFBG sensors open up a multitude of opportunities for single-point biomedical sensing in hard-to-reach spaces, and offer an extremely improved LOD level to molecular interactions together with very controllable cross-sensitivities (Voisin et al., 2014; Lepinay et al., 2014; Shevchenko et al., 2014).

It is the purpose of this paper to demonstrate the intrinsic relationship between protein outflow (induced by adriamycin nephropathy) and RI variation (over the range of 1.3400–1.3408 approximately) in urine by simply using an in-fiber based, label-free direct detection device. This particular TFBG configuration has been optimized with an especially designed metal coating that allows both SPR excitation and conventional evanescent field probing of the medium refractive index, thereby enabling a novel differential data analysis method which increases the protein concentration sensitivity of 5.5 dB/(mg/ml) and a limit of detection of 1.5×10^{-3} mg/ml over repeated measurement of rat urinary samples with different concentration of protein. The detection process was precisely controlled with a micro-fluidic chip which allows the measurement of μL-volumes of bio-sample solutions. The proposed in-fiber plasmonic biosensor shows a minimal cross-sensitivity to temperature (through referencing of the spectrum by the core mode resonance) and its fabrication (UV-light grating-inscription and surface nanometric-coating) does not impact the structural integrity of the fiber so as to ensure the sensing stability and reproducibility. Finally, our study on the relationship between the outflow of protein and RI variation in urine will be helpful to the understanding and evaluation of adriamycin nephropathy (Okuda et al., 1986; Jeyaseelan et al., 2006).

2. Materials and methods

2.1. Bio-samples preparation

The schematic of the pharmacological process of adriamycin nephropathy and of the urine detection with a fiber-optic sensor

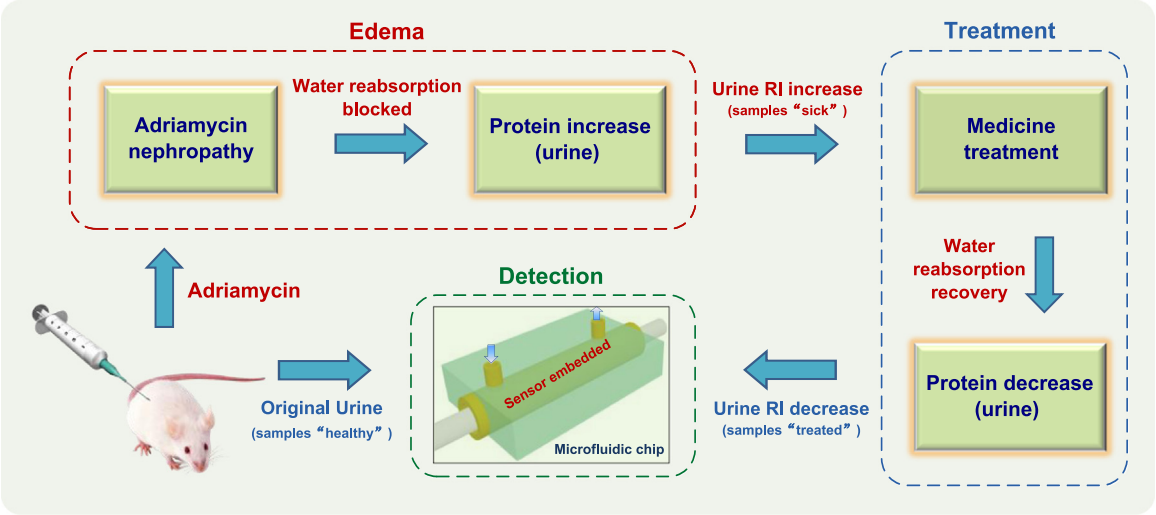

Fig. 1. Schematic of the pharmacological process of adriamycin nephropathy and of the urine detection with a fiber-optic sensor embedded in a microfluidic chip.

embedded in a microfluidic chip is shown in Fig. 1.

Experimental animals: healthy male rats of specific pathogen free level, age of 6–8 weeks, weight of 200 ± 20 g, and total number of 30, are purchased from the experimental animal center of Guangdong University of Chinese Medicine (Certification No. 44005900000273). The rats were raised in SPF level animal rooms (temperature of 22–25 °C, humidity of 40–70%). All the operations are strictly executed in accordance with the experimental animal agreement of the Chinese medicine academy committee.

Adriamycin: with a trade name of Doxorubicin, was purchased from Shenzhen Main Luck Pharmaceuticals Inc., China.

ZhenWuTang medicine: a traditional Chinese prescription used for adriamycin nephropathy treatment. It contains poria, herbaceous peony, rhizoma atractylodis macrocephalae, ginger and aconite (with the proportion of 9:9:6:9:4). All of the above mentioned Chinese herbs were processed by Guangdong Kangmei Pharmaceutical Inc., China.

Experimental process: all the rats were randomly divided into three groups (10 rats for each group): (1) no adriamycin nephropathy group (healthy group), in which the healthy rats were injected with glucose saline (1 ml once) and then injected with distilled water (1 ml/100 mg per day) for 4 weeks, this group is used for comparison; (2) adriamycin nephropathy group (sick group), in which the healthy rats were injected with adriamycin (5 mg/kg once) and then injected with distilled water (1 ml/100 mg per day) for 4 weeks; (3) Zhenwutang treatment group (treated group), in which the healthy rats were injected with adriamycin (5 mg/kg once) and then with ZhenWuTang medicine (19 g/kg per day) for 4 weeks. After the completion of the above process, the urine of the rats for each group were collected and used for testing with our proposed plasmonic fiber-optic sensing method. The traditional BCA method was also used on the same samples for comparison.

2.2. Experimental setup and optical configuration

The experimental setup requires the sensor to operate in the transmission regime (Fig. 2). During the experiments, the 125 μm-diameter sensors were fixed in PDMS-based micro-fluidic channels designed specifically for the biosensing tests (Guo et al., 2014). While each individual sensor was fixed in the micro-channel (width 200 μm by height 150 μm) with help of UV-sensitive adhesive on both sides of the sensing element, thus delimiting a length of 20 mm (for a total sensing volume of 35 μL, taking into account the volume taken up by the fiber). Three groups of urine sample solutions (Fig. 2a) corresponding to above mentioned "no adriamycin nephropathy group (healthy group)", "adriamycin nephropathy group (sick group)" and "Zhenwutang treatment group (treated group)" were prepared for detection and analysis. Urinary sample solutions were injected into the micro-fluidic chip (Fig. 2b) via an electronic-controlled pump, eliminating potential environmental effects (strain, pressure, bending, humidity, etc.).

The plasmonic TFBG sensing probe was excited by a broadband light source (BBS) launched in the fiber core covering the spectral region from 1440 to 1560 nm, and its transmission spectrum monitored by an optical spectrum analyzer (OSA) with minimum wavelength resolution of 0.02 nm. A linear polarizer and polarization controller (PC) were placed upstream of the TFBG probe to adjust and orient the state of polarization of the light launched into fiber grating so as to provide the strongest SPR excitation, i.e. selective excitation of cladding modes with almost 100% radially polarized light at the cladding surface, i.e. perpendicular to the metal surface.

3. Plasmonic TFBG sensor

3.1. Fabrication of TFBG

The TFBG sensor (15 mm in length) was manufactured using the phase-mask technique in a commercial single-mode fiber (Fig. 3a). The fabrication process mainly includes the following three steps. Firstly, the fiber was hydrogen-loaded (temperature: 50 °C, pressure: 1500 psi, loading time: 168 h) to increase the photosensitivity of the fiber core. Secondly, pulsed 193 nm UV light (power of 3 mJ per pulse, frequency of 200 Hz) was focused with a cylinder lens and scanned over the fiber region. The phase

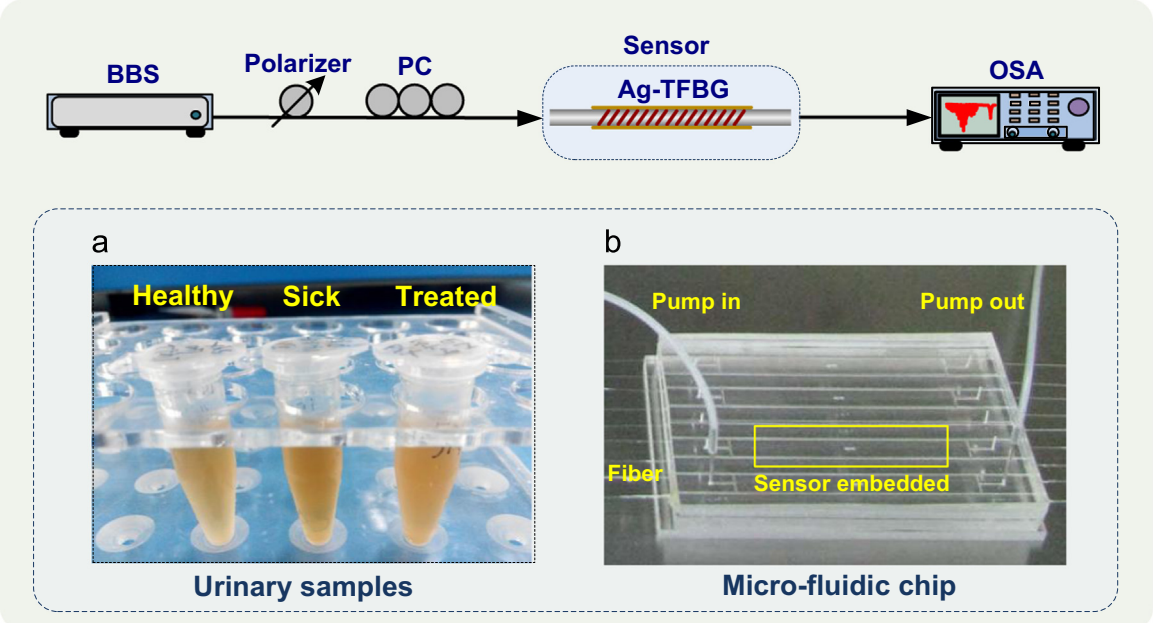

Fig. 2. Schematic of fiber-optic sensing system: (a) urinary samples with different concentration of proteins; (b) micro-fluidic chip for urinary samples measurement.

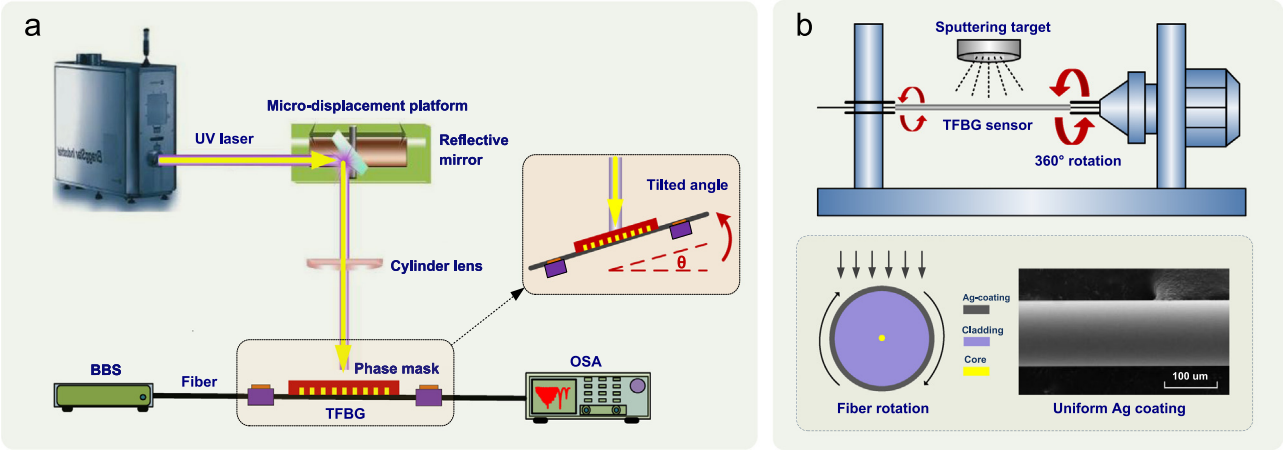

Fig. 3. Schematics of (a) TFBG inscription system and (b) surface nanometric-coating system ((I) fiber rotated instead of fixed and (II) photograph of uniform Ag coating).

mask divides the laser beam into ± 1 order diffraction orders so as to induce a periodical effective refractive index modulation in the fiber core. Finally, by rotating the phase mask and the fiber (inset of Fig. 3a) simultaneously, a selectable tilt angle (relatively to the longitudinal axis of the fiber) can be easily induced into the grating. The tilt of the grating is an important parameter that can be used to choose which set of cladding modes is to be excited. As a result, it makes it possible to adjust the operating range of the sensor in order to optimize the response for certain refractive indices. Here, the tilt angle of TFBG was selected to be 20 °, which provides the maximal amplitude of cladding modes for aqueous solutions measurement (RI range of 1.32–1.35).

3.2. Ultra-thin metallic coating

A ultra-thin silver film was deposited on the fiber probe using the sputtering technique (RF magnetron sputtering). To achieve a high quality coating, two issues must be noted. One is to improve the film's adhesion. Here we use a 2–3 nm thickness of chromium sandwiched between the optical fiber surface and the silver film. The second is to ensure a uniform thickness of silver film over the whole fiber surface. Traditional flat-plane sputtering technique is not fit for the small diameter cylindrical fiber because sputtering is directional from the fixed target. To avoid thickness non-uniformities, during the sputtering process the fiber was rotated along its axis (Fig. 3a). With this design, we can ensure a very uniform nanometric coating over fiber surface (Fig. 3b).

3.3. Hybrid plasmonic and cut-off resonances excitations

The key point of achieving differential spectral changes between the SPR mode and a near cut-off cladding mode with a single coated TFBG is to choose a proper thickness of the nanometric-coating. Fig. 4 shows the schematic diagrams and spectral characteristics of the same TFBG with different thicknesses of Ag on its surface with: no coating, 20–30 nm and 50 nm Ag-coating respectively. We will show in the next paragraphs how the different coating thicknesses lead to different sensing characteristics. Note that all the spectra shown in Fig. 4 are measured from the same TFBG in the same water solution (RI = 1.332).

For the bare TFBG (Fig. 4a), the surrounding RI measurement is based on evanescent wave (EW) of cladding modes. Beside the core mode located at the longest wavelength (immune to surrounding RI), there are hundreds of cladding-guided resonances with high sensitivity to surrounding RI and tens of leaky modes with effective indices larger than the surrounding RI. The boundary between cladding and leaky modes is indicated by a sudden increase in the loss of the modes, evidenced by reduced amplitude of the cladding mode resonance (the red asterisk "*" marked in Fig. 4a). The most sensitive cladding mode is the last one remaining guided for a given surrounding RI because it is the mode with the largest penetration outside the fiber (Guo et al., 2014).

For the "thick" Ag-coating TFBG (Fig. 4c), the surrounding RI measurement is based on the excitation of a surface plasmon wave (SPW). In TFBGs, when linearly polarized light is launched with its polarization parallel to the tilt plane (P-polarized), the electric field of the cladding modes is nearly 100% polarized in the radial direction, i.e. in the TM polarization relative to the metal coating. Evidence of SPR in the spectrum for this polarization is the disappearance of the cladding mode resonances near 1490 nm due to the coupling of the cladding mode energy to the very lossy SPW at these wavelengths. This coupling is maximized for thicknesses near 50 nm. When the other direction of the input polarized light is used, i.e. the S-polarization, the electric field is aligned in the TE direction with the fiber surface and no SPR can occur. Using the TM spectrum, the fine comb of narrowband resonances of the TFBG provides a unique tool to measure small shifts of the plasmon with high accuracy. This is accomplished by choosing a resonance on the short wavelength side of the maximum SPR attenuation (the red asterisk "*" marked in Fig. 4c, named plasmonic resonance). The shift of the SPR can be easily measured by monitoring the amplitude change of the chosen resonance, as it increases when the SPR moves away (towards longer wavelengths when the surrounding RI increases) or decreases when the SPR approaches in response to a decreasing RI (Caucheteur et al., 2013).

Finally, the "thin" Ag-coating TFBG (Fig. 4b) provides a trade-off condition to combine the two methodologies in a single device. Through experiments with fibers coated by various thicknesses between 0 and 50 nm, it was found that the 20–30 nm thickness range can support a slightly weakened SPR excitation and that it also allows some cladding modes near cut-off to tunnel across the metal film (two modes identified by red asterisks "*" in Fig. 4b). Because both of these two resonances show extremely high RI sensitivities but inverse amplitude responses to the surrounding RI (Section 4 makes this determination clear), such ultra-thin coating design will further improve the limit of detection by using a differential amplitude measurement instead of an absolute one.

4. Results and discussion

Fig. 5 presents the spectral response of the experimental tests and corresponding data analysis. The proposed biosensor shows a quick response (1.0 s per full scan by the OSA) and clearly

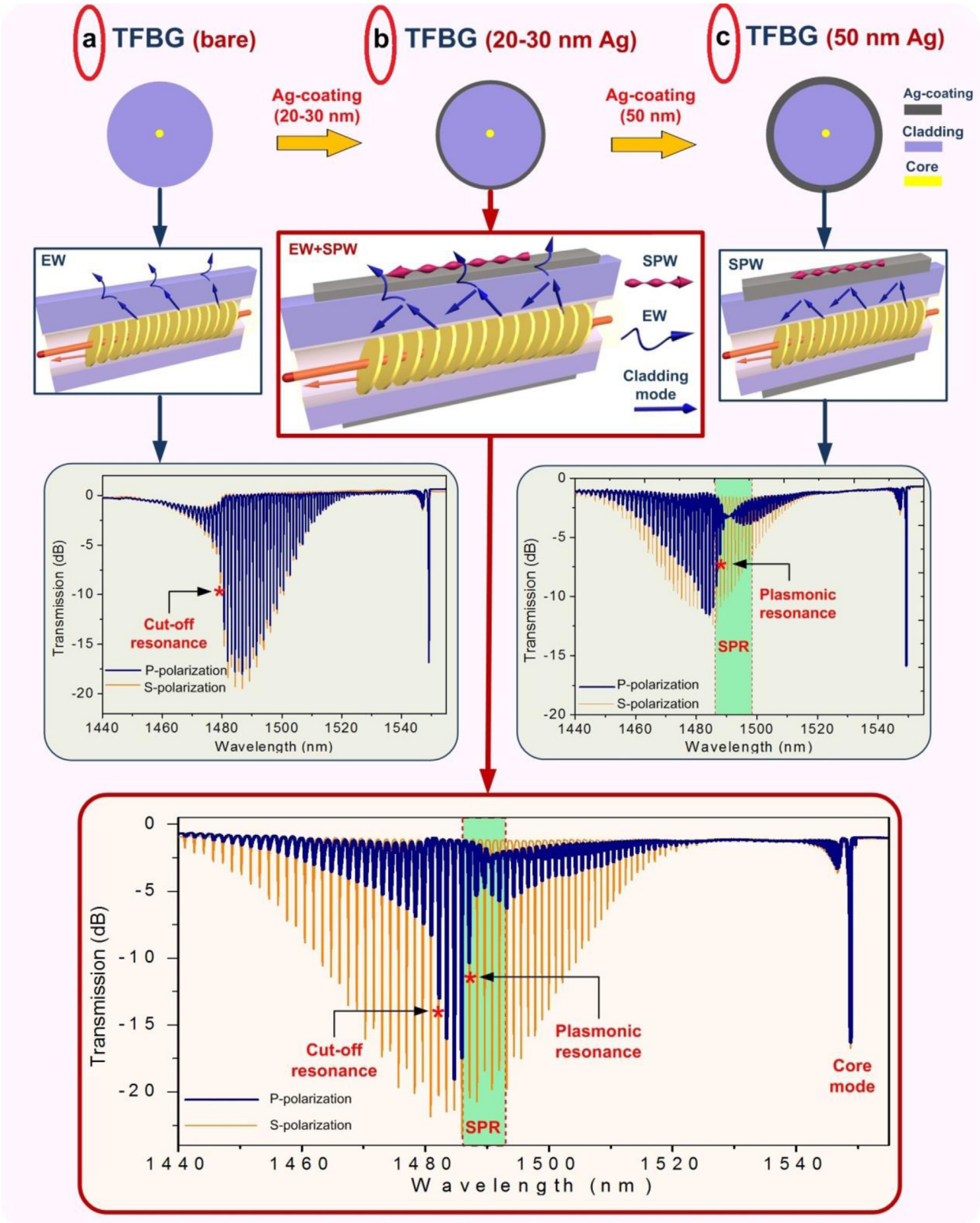

Fig. 4. Spectral characteristics of TFBG (20° tilted angle) versus different thickness of nanometric-coating: (a) bare TFBG without Ag-coating (a clear cut-off resonance at the boundary between guided modes (at longer wavelength side) and leaky modes (at shorter wavelength side)); (b) TFBG with 20–30 nm Ag-coating (hybrid "cut-off" and "plasmonic" resonances achieved simultaneously over a single TFBG); (c) TFBG with 50 nm Ag-coating (the normal thickness range for "plasmonic" excitation without leaky modes (at shorter wavelength side)). Note: red stars mark the corresponding position of "cut-off" and "plasmonic" resonances; P and S polarizations corresponds to two orthogonal polarizations in which SPR excitation over the P polarization; All above transmission spectra are measured from one TFBG in the same water solution (RI = 1.332). (For interpretation of the references to color in this figure legend, the reader is referred to the web version of this article.)

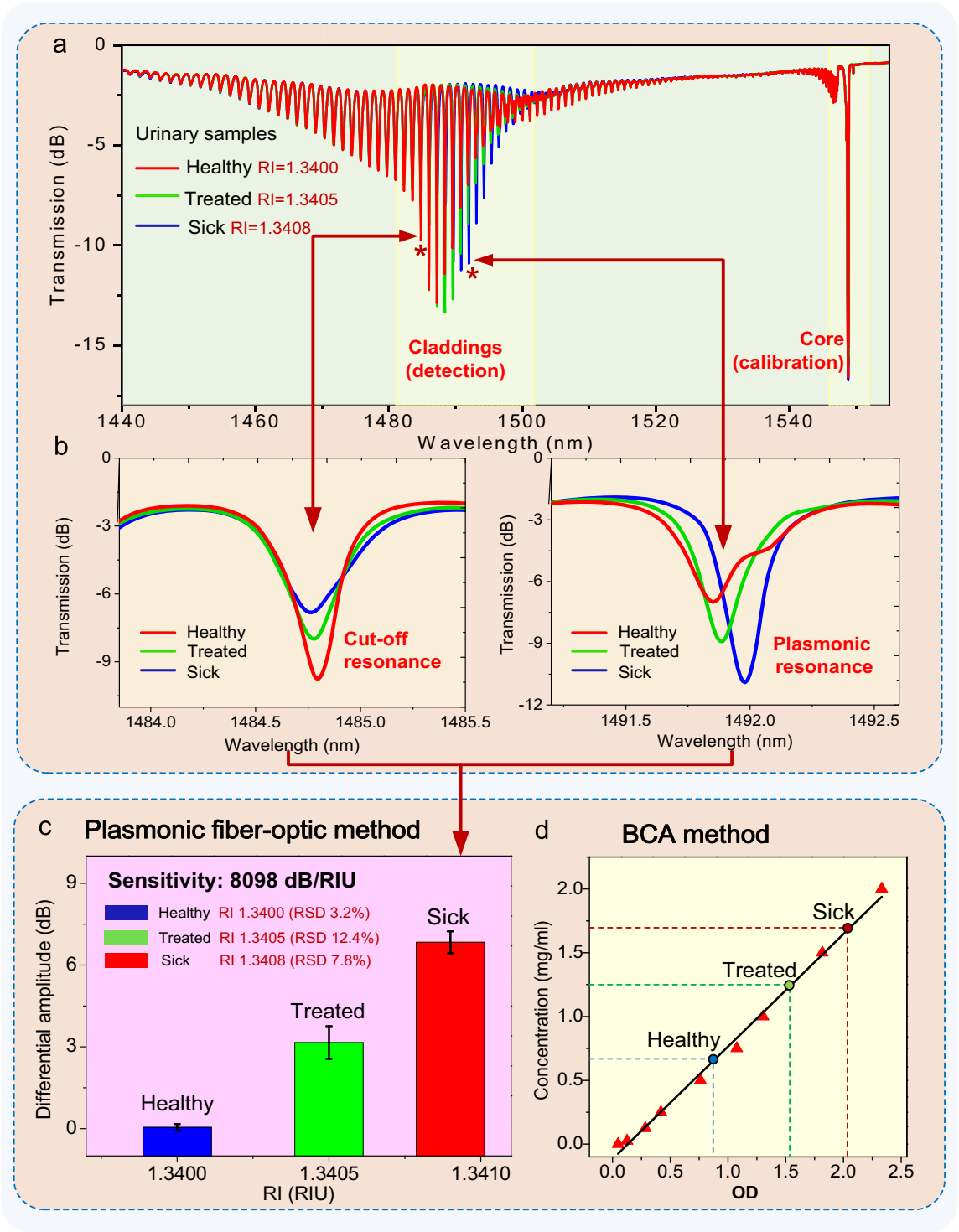

Fig. 5. Urinary samples detection results based on our "proposed" plasmonic TFBG sensor (a–c) and "traditional" type analytic biochemistry assays (d): (a) the whole spectral responses; (b) zoomed-in spectral responses of "cut-off" and "plasmonic" resonances used for sensing; (c) statistical sensing results of urinary samples over repeat measurement for three group of rats (healthy, sick and treated); (d) standard curve of the whole protein concentration achieved by the BCA method. (For interpretation of the references to color in this figure, the reader is referred to the web version of this article.)

identified spectral signature for different rat urinary samples: the "healthy group", "sick group" and "treated group".

In more detail, Fig. 5a shows the whole transmission spectra of the sensor. It provides two important pieces of information: one is that very small surrounding RI perturbations induce significant changes in the cladding mode resonances (such changes could arise from bulk medium changes, thickness changes in an adlayer, or molecular binding events for functional layers attached to the metal surface). The other is the temperature self-calibration ability indicated by the unchanged core mode (where spectral shifts due to temperature changes can be eliminated by referencing all wavelengths to the core mode, which is unaffected by the surrounding RI and has the same temperature dependence with the other modes, thereby ensuring that the differential spectra are due solely to surrounding RI changes or different bio-sample solutions).

Fig. 5b presents the zoomed spectral responses of the marked cut-off resonance and of the plasmonic resonance. Obviously, both of these resonances show high sensitivity (several dB of change) but inverse amplitude responses to the near surface RI. As already briefly mentioned, when the surrounding RI increases, the SPR attenuation shifts towards the longer wavelength side and the marked plasmonic resonance amplitude recovers to its original "sharp" state so as to get stronger. The cut-off resonance however decreases its amplitude because the surrounding RI increase brings the resonance even closer to cut off and therefore decreases its amplitude. By using a differential amplitude monitoring between cut-off and plasmonic resonances (Fig. 5c), the effect of proteins in the urine of rats with different concentrations (related to the "healthy", "sick" and "treated" rat groups) and corresponding RI ranging from 1.3400 to 1.3408 (the refractive indices of the solutions were measured at a wavelength of 589 nm with an Abbe refractometer) were clearly discriminated in-situ with an amplitude variation sensitivity of 8100 dB/RIU and a limit of detection of 10^{-5} RIU (the refractive indices at the wavelength of operation of the sensor are different but this has no impact on the measurement, following sensor calibration for a given application). Repeat measurements were used to identify these performance indicators with a relative standard deviation (RSD) of less than 15% (the average and error bars shown in Fig. 5c were determined from three measurements of 30 samples (10 samples for each group)).

Our method has also been compared with the traditional BCA method (in which the concentration of proteins is determined by the amount of light absorption at 562 nm, named as optical density (OD), arising from the reaction of proteins in copper salt solutions), for which all the experimental conditions used are the same. The BCA results (red triangle data) shown in Fig. 5d provide the measurement of the total concentration of the protein in the rat urine samples and with these data a standard curve of the whole protein concentration can be achieved (black line). Such standard curve is necessary for the calibration of the fiber result (i.e. refractive index change vs. protein concentration, using the three fiber-optic measurements (the colored circle points marked in Fig. 5d)). Calibrated with the traditional BCA method (Fig. 5d), our proposed plasmonic fiber-optic sensor provides an protein concentration sensitivity of 5.5 dB/(mg/ml) and a limit of detection of 1.5×10^{-3} mg/ml.

5. Conclusions

In summary, the feasibility of highly sensitive detection of proteinuria using plasmonic tilted fiber grating sensors with ultrathin nanometric-coating has been demonstrated. By using a differential amplitude monitoring between the plasmonic and cut-off resonances, a protein concentration sensitivity of 5.5 dB/(mg/ml) and a limit of detection of 1.5×10^{-3} mg/ml have been achieved. The intrinsic relationship between the outflow of protein and RI variation in urine has been demonstrated, which helps to the evaluation and development of new drugs for nephropathy treatment. The detection process was precisely controlled with a micro-fluidic chip which allows the measurement work on submicroliter dose of bio-sample solutions. For bio-chemical applications with high specificity, the nanometric-coated TFBG can be used for label-free sensing when provided with a functionalized coating whose RI can be modified by the selective attachment of certain types of molecules or cells. The sensor can operate in reflection (instead of transmission) with a cleaved end downstream of the grating and with gold or silver coating on the face of the cleave. It makes the length of the entire sensor "head" very small (as little as 10 to 20 mm) so that the sensing probe can be easily inserted into the media to be sensed. The proposed in-fiber plasmonic biosensor shows a minimal cross-sensitivity to temperature and its fabrication does not impact the structural integrity of the fiber, makes it an appealing solution for rapid, low consumption and highly sensitive detection of analytes at low concentrations in medicine, chemical and environmental monitoring.

Acknowledgments

This work was funded by the National Natural Science Foundation of China (Nos. 61205080, 61225023, 51403077 and 81173378), the Research Project for Practice Development of National TCM Clinical Research Bases (No. JDZX2012012), the Guangdong Natural Science Foundation of China (No. 2014A030313387), the Youth Science and Technology Innovation Talents of Guangdong (No. 2014TQ01 × 539), the Fundamental Research Funds for the Central Universities of China (No. 21615446). J. Albert acknowledges the support of the Natural Sciences and Engineering Research Council of Canada (No. RGPIN 2014-05612) and the Canada Research Chairs Program (No. 950-217783).

References

Ishani, A., Grandits, G.A., Grimm, R.H., Svendsen, K.H., Collins, A.J., Prineas, R.J., Neaton, J.D., 2006. Association of single measurements of dipstick proteinuria, estimated glomerular filtration rate, and hematocrit with 25-year incidence of end-stage renal disease in the multiple risk factor intervention trial. J. Am. Soc. Nephrol. 17, 1444–1452.

Tonelli, M., Muntner, P., Lloyd, A., Manns, B.J., James, M.T., Klarenbach, S., Quinn, R. R., Weibe, N., Hemmelgarn, B.R., 2011. Using proteinuria and estimated glomerular filtration rate to classify risk in patients with chronic kidney disease: a cohort study. Ann. Intern. Med. 154, 12–21.

Agrawal, V., Marinescu, V., Agarwal, M., McCullough, P.A., 2009. Cardiovascular implications of proteinuria: an indicator of chronic kidney disease. Nat. Rev. Cardiol. 6, 301–311.

Matsushita, K., Velde, M., Astor, B.C., Woodward, M., Levey, A.S., Jong, P.E., Coresh, J., 2010. Association of estimated glomerular filtration rate and albuminuria with all-cause and cardiovascular mortality in general population cohorts: a collaborative meta-analysis. Lancet 375, 2073–2081.

Chial, H.J., Thompson, H.B., Splittgerber, A.G., 1993. A spectral study of the charge forms of coomassie blue G. Anal. Biochem. 209, 258–266.

Smith, P.K., Krohn, R.I., Hermanson, G.T., Mallia, A.K., Gartner, F.H., Provenzano, M. D., Fujimoto, E.K., Goeke, N.M., Olson, B.J., Klenk, D.C., 1985. Measurement of protein using bicinchoninic acid. Anal. Biochem. 150, 76–85.

Baldini, F., Brenci, M., Chiavaioli, F., Giannetti, A., Trono, C., 2012. Optical fibre gratings as tools for chemical and biochemical sensing. Anal. BioAnal. Chem. 402, 109–116.

Wang, X.D., Wolfbeis, O.S., 2013. Fiber-optic chemical sensors and biosensors (2008–2012). Anal. Chem. 85, 487–508.

White, I.M., Fan, X.D., 2008. On the performance quantification of resonant refractive index sensors. Opt. Express 16, 1020–1028.

Homola, J., 2008. Surface plasmon resonance sensors for detection of chemical and biological species. Chem. Rev. 108, 462–493.

Piliarik, M., Homola, J., 2009. Surface plasmon resonance (SPR) sensors: approaching their limits? Opt. Express 17, 16505–16517.

Shalabney, A., Abdulhalim, I., 2011. Sensitivity-enhancement methods for surface plasmon sensors. Laser Photon- Rev. 5, 571–606.

Caucheteur, C., Guo, T., Albert, J., 2015. Review of plasmonic fiber optic biochemical sensors: improving the limit of detection. Anal. BioAnal. Chem. 407, 3883–3897.

Albert, J., Shao, L.Y., Caucheteur, C., 2013. Tilted fiber Bragg grating sensors. Laser Photon Rev. 7, 83–108.

Guo, T., Liu, F., Guan, B.O., Albert, J., 2016. Tilted fiber grating mechanical and biochemical sensors. Opt. Laser Technol. 78, 19–33.

Thomas, J.U., Jovanovic, N., Krämer, R.G., Marshall, G.D., Withford, M.J., unnermann, A.T., Nolte, S., Steel, M.J., 2012. Cladding mode coupling in highly localized fiber Bragg gratings II: complete vectorial analysis. Opt. Express 20, 21434–21449.

Caucheteur, C., Voisin, V., Albert, J., 2013. Polarized spectral combs probe optical fiber surface plasmons. Opt. Express 21, 3055–3066.

Guo, T., Liu, F., Liu, Y., Chen, N.K., Guan, B.O., Albert, J., 2014. In-situ detection of density alteration in non-physiological cells with polarimetric tilted fiber grating sensors. Biosens. Bioelectron. 55, 452–458.

Voisin, V., Pilate, J., Damman, P., Mégret, P., Caucheteur, C., 2014. Highly sensitive detection of molecular interactions with plasmonic optical fiber grating

sensors. Biosens. Bioelectron. 51, 249–254.
Lepinay, S., Staff, A., Ianoul, A., Albert, J., 2014. Improved detection limits of protein optical fiber biosensors coated with gold nanoparticles. Biosens. Bioelectron. 52, 337–344.
Shevchenko, Y., Camci-Unal, G., Cuttica, D.F., Dokmeci, M.R., Albert, J., Khademhosseini, A., 2014. Surface plasmon resonance fiber sensor for real-time and label-free monitoring of cellular behavior. Biosens. Bioelectron. 56, 359–367.
Okuda, S., Oh, Y., Tsuruda, H., Onoyama, K., Fujimi, S., Fujishima, M., 1986. Adriamycin-induced nephropathy as a model of chronic progressive glomerular disease. Kidney Int. 29, 502–510.
Jeyaseelan, K., Sepramaniam, S., Armugam, A., Wintour, E.M., 2006. Aquaporins: a promising target for drug development. Expert. Opin. Ther. Targets 10, 889–909.
Guo, J.H., Li, C.M., Kang, Y.J., 2014. PDMS-film coated on PCB for AC impedance sensing of biological cells. Biomed. Microdevices 16, 681–686.